Microwave Doppler spectra of sea return at small incidence angles: specular point scattering contribution*

Zhang Yan-Min(张彦敏)[a], Wang Yun-Hua(王运华)[b]†, and Zhao Chao-Fang(赵朝方)[b]

[a] *Department of Physics, Ocean University of China, Qingdao* 266100, *China*
[b] *Ocean Remote Sensing Institute, Ocean University of China, Qingdao* 266003, *China*

(Received 20 December 2009; revised manuscript received 25 January 2010)

It is well known that the sea return echo contains contributions from at least two scattering mechanisms. In addition to the resonant Bragg scattering, the specular point scattering plays an important role as the incidence angle becomes smaller ($\leq 20°$). Here, in combination with the Kirchhoff integral equation of scattering field and the stationary phase approximation, analytical expressions for Doppler shift and spectral bandwidth of specular point scattering, which are insensitive to the polarization state, are derived theoretically. For comparison, the simulated results related to the two-scale method (TSM) and the method of moment (MOM) are also presented. It is found that the Doppler shift and the spectral bandwidth given by TSM are insufficient at small incidence angles. However, a comparison between the analytical results and the numerical simulations by MOM in the backscatter configuration shows that our proposed formulas are valid for the specular point scattering case. In this work, the dependences of the predicted results on incidence angle, radar frequency, and wind speed are also discussed. The obtained conclusions seem promising for a better understanding of the Doppler spectra of the specular point scattering fields from time-varying sea surfaces.

Keywords: Doppler spectrum, specular point scattering, sea surface, Kirchhoff approximation

PACC: 4120, 4110H

1. Introduction

Doppler spectrum of a radar signal backscattered from ocean surface reflects the distribution of the line-of-sight velocity of the scattering facets. The first moment of the Doppler spectrum, i.e. Doppler shift, corresponds to a power-weighted mean velocity of the facets.[1−3] And the bandwidth of the spectrum is determined by the variance of the scatterer velocity directly.[1,2] Although the microwave Doppler spectrum can carry more information about the sea state than the scattering coefficient (NRCS), the investigations on this subject are relatively less so far. In Refs. [4]–[6], the spectral properties of microwave backscattered signal from time-varying oceanic surfaces were investigated numerically based on the MOM. The simulation results from distinct hydrodynamic sea surface model were compared by Topokov *et al.* In Refs. [7] and [8], Doppler shifts of backscattered fields from linear sea surfaces were predicted by asymptotic electromagnetic wave scattering theories. As pointed out by Mouche *et al.*,[7] the predicted Doppler shifts for the Kirchhoff and the first order small slope approximations (SSA-I) in co-polarized configuration are independent of polarization state. On the other hand, the local curvature solutions yield a significant difference between co-polarized predicated Doppler shifts. In Ref. [9], the Doppler properties of radar echoes from the nonlinear Gerstner's sea surface were analysed by the SSA-I, and some significant conclusions were obtained. However, it is a pity that few convenient formulas for Doppler shift and bandwidth were obtained in Refs. [4]–[9]. At moderate- and low-grazing angles, the Doppler spectrum calculations based on the composite sea surface model (the two-scale model (TSM)) and a comparison with experimental data were reported in Refs. [10] and [11]. However, if the incident angle is smaller than 20°, the spectral model given by TSM is insufficient because the Bragg-scattering mechanism is invalid. At small incidence angles, the specular point scattering will play an important role and the form of the spectrum should be changed by the quasi-reflective field.

In this work, Doppler properties of a radar sig-

*Project supported by the Young Scientists Fund of the National Natural Science Foundation of China (Grant No. 40906088), and the Specialized Research Fund for the Doctoral Program of Higher Education, China (Grant No. 200804231021).
†Corresponding author. E-mail: wyh78917@yahoo.com.cn
© 2010 Chinese Physical Society and IOP Publishing Ltd

nal reflected from time-varying sea surface are studied by utilizing the Kirchhoff approach and the stationary phase approximation.[12] Analytical expressions for Doppler shift and spectral bandwidth of specular point scattering are derived theoretically. The rest of the present paper is organized as follows. In Section 2, based on the Kirchhoff approach and the stationary phase approximation, the formula for predicting Doppler shift is derived analytically. In Section 3, the spectral bandwidth model for specular point scattering is presented, while the results and the comments are given in Section 4. The concluding remarks and perspectives are provided in Section 5.

2. Doppler shift of specular point scattering

Using the Kirchhoff approach, the scattering field can be written in terms of the tangential field on a rough surface. The surface field is then approximated by the field that would be present if the rough surfaces were replaced by a planar surface tangential to the point of interest. With this assumption, the scattered field for one-dimensional surface can be expressed by the following integral equation:[12]

$$\begin{aligned}\boldsymbol{E}^{\mathrm{s}} = {} & K\hat{\boldsymbol{n}}_{\mathrm{s}} \times \int [\hat{\boldsymbol{n}} \times \boldsymbol{E} - \eta \hat{\boldsymbol{n}}_{\mathrm{s}} \times (\hat{\boldsymbol{n}} \times \boldsymbol{H})] \\ & \times \exp[\mathrm{i}k(\hat{\boldsymbol{n}}_{\mathrm{s}} - \hat{\boldsymbol{n}}_{\mathrm{i}}) \cdot \boldsymbol{l}'] \mathrm{d}\boldsymbol{l}', \end{aligned} \tag{1}$$

where $K = \sqrt{\mathrm{i}k/8\pi R_0}\exp(-\mathrm{i}kR_0)$, k denotes the wave number of the incident field, η is the wave impedance in free space, R_0 is the distance from the centre of the illuminated surface to the point of observation, $\hat{\boldsymbol{n}}_{\mathrm{i}}$ and $\hat{\boldsymbol{n}}_{\mathrm{s}}$ are the unit vectors in the incident and the scattered directions respectively, defined as

$$\hat{\boldsymbol{n}}_{\mathrm{i}} = \sin\theta_{\mathrm{i}}\hat{\boldsymbol{x}} - \cos\theta_{\mathrm{i}}\hat{\boldsymbol{z}}, \tag{2}$$

$$\hat{\boldsymbol{n}}_{\mathrm{s}} = \sin\theta_{\mathrm{s}}\hat{\boldsymbol{x}} + \cos\theta_{\mathrm{s}}\hat{\boldsymbol{z}}, \tag{3}$$

where $\hat{\boldsymbol{x}}$ and $\hat{\boldsymbol{z}}$ are both unit vectors in Cartesian coordinates, $\boldsymbol{l}' = x'\hat{\boldsymbol{x}} + z'\hat{\boldsymbol{z}}$ is the vector denoting the location of the surface point according to the centre of the sea surface $z'(x', t)$, t denotes the time related to the variation of sea surface. For the incident field with unit amplitude, in Eq. (1), the total $\hat{\boldsymbol{n}} \times \boldsymbol{E}$ electric and magnetic $\hat{\boldsymbol{n}} \times \boldsymbol{H}$ tangential fields are given by[12]

$$\begin{aligned}\hat{\boldsymbol{n}} \times \boldsymbol{E} = {} & [(1 + R_{\mathrm{H}})(\hat{\boldsymbol{a}} \cdot \hat{\boldsymbol{b}})(\hat{\boldsymbol{n}} \times \hat{\boldsymbol{b}}) \\ & - (1 - R_{\mathrm{V}})(\hat{\boldsymbol{n}} \cdot \hat{\boldsymbol{n}}_{\mathrm{i}})(\hat{\boldsymbol{a}} \cdot \hat{\boldsymbol{d}})\hat{\boldsymbol{b}}]E_0, \end{aligned} \tag{4}$$

$$\begin{aligned}\hat{\boldsymbol{n}} \times \boldsymbol{H} = {} & -[(1 + R_{\mathrm{V}})(\hat{\boldsymbol{a}} \cdot \hat{\boldsymbol{d}})(\hat{\boldsymbol{n}} \times \hat{\boldsymbol{b}}) \\ & + (1 - R_{\mathrm{H}})(\hat{\boldsymbol{n}} \cdot \hat{\boldsymbol{n}}_{\mathrm{i}})(\hat{\boldsymbol{a}} \cdot \hat{\boldsymbol{t}})\hat{\boldsymbol{b}}]E_0/\eta, \end{aligned} \tag{5}$$

where $\hat{\boldsymbol{a}}$ is the unit polarization vector of the incident field, $\hat{\boldsymbol{n}}$ is the unit vector normal to the local surface defined as $\hat{\boldsymbol{n}} = (-\partial z'/\partial x'\hat{\boldsymbol{x}} + \hat{\boldsymbol{z}})/\sqrt{1 + (\partial z'/\partial x')^2}$, $\hat{\boldsymbol{b}}$ and $\hat{\boldsymbol{d}}$ are given by $\hat{\boldsymbol{b}} = \hat{\boldsymbol{n}}_{\mathrm{i}} \times \hat{\boldsymbol{n}}/\|\hat{\boldsymbol{n}}_{\mathrm{i}} \times \hat{\boldsymbol{n}}\|$ and $\hat{\boldsymbol{d}} = \hat{\boldsymbol{n}}_{\mathrm{i}} \times \hat{\boldsymbol{b}}$ respectively, $\{R_{\mathrm{V}},\ R_{\mathrm{H}}\}$ denote the Fresnel coefficients in the vertical V and horizontal H polarizations determined by local incident angle $\theta'_{\mathrm{i}} = \arccos[\hat{\boldsymbol{n}} \cdot \hat{\boldsymbol{n}}_{\mathrm{i}}]$, and E_0, which is assumed to be 1, is the amplitude of the incident field. From Eqs. (4) and (5), it is found that the integrand of Eq. (1) depends on deterministic variable x' and two random variables, i.e. $\{z', \partial z'/\partial x'\}$. At low incident angles, to solve the Kirchhoff integral equation analytically, the stationary phase method can be utilized. This method is valid when both the radius of curvature at each point of the surface and the correlation length are larger than the incident electromagnetic wavelength. In the stationary phase method it is assumed that the major contributions of the scattered field from the sea surface come from regions around the specular points. And these specular points are determined by

$$S = \frac{\partial z'}{\partial x'} = \frac{\sin\theta_{\mathrm{i}} - \sin\theta_{\mathrm{s}}}{\cos\theta_{\mathrm{i}} + \cos\theta_{\mathrm{s}}}. \tag{6}$$

Using Eq. (6), in the integral of Eq. (1), $(\hat{\boldsymbol{n}} \times \boldsymbol{E} - \eta\hat{\boldsymbol{n}}_{\mathrm{s}} \times \hat{\boldsymbol{n}} \times \boldsymbol{H})$ would be no longer a function of integration variable $\boldsymbol{l}'$. Thus scattered field $E^{\mathrm{s}}_{\mathrm{pq}}$ can be expressed as[12]

$$\boldsymbol{E}^{\mathrm{s}}_{\mathrm{pq}} = K\boldsymbol{U}_{\mathrm{pq}}I_{\mathrm{SP}}, \tag{7}$$

where subscript pq denote $H_{\mathrm{s}}H_{\mathrm{i}}$ or $V_{\mathrm{s}}V_{\mathrm{i}}$, and $\{H_{\mathrm{s}}, V_{\mathrm{s}}, H_{\mathrm{i}}, V_{\mathrm{i}}\}$ represents horizontal or vertical polarization for the scattered and the incident fields, $\boldsymbol{U}_{\mathrm{pq}}$ and I_{SP} can be written as

$$\boldsymbol{U}_{\mathrm{pq}} = \hat{\boldsymbol{n}}_{\mathrm{s}} \times (\hat{\boldsymbol{n}} \times \boldsymbol{E} - \eta\hat{\boldsymbol{n}}_{\mathrm{s}} \times \hat{\boldsymbol{n}} \times \boldsymbol{H}) \tag{8a}$$

and

$$I_{\mathrm{SP}} = \int \exp[\mathrm{i}k(\hat{\boldsymbol{n}}_{\mathrm{s}} - \hat{\boldsymbol{n}}_{\mathrm{i}}) \cdot \boldsymbol{l}'] \mathrm{d}\boldsymbol{l}' \tag{8b}$$

respectively.

It is well known that the scattering coefficient for an extended target is defined as

$$\sigma_{\mathrm{pq}} = \frac{2\pi R_0 \left\langle \left| \boldsymbol{E}^{\mathrm{s}}_{\mathrm{pq}} \right|^2 \right\rangle}{L_0 \left| \boldsymbol{E}_{\mathrm{i}} \right|^2}, \tag{9}$$

where L_0 denotes the length of the illuminated one-dimensional (1D) surface. Substituting Eq. (7) into

Eq. (9), after a lengthy but straightforward manipulation, the scattering coefficient $\sigma_{\rm pq}$ from the time-varying one-dimensional sea surface can be obtained as[12]

$$\sigma_{\rm pq} = \frac{kQ^2}{4Q_z^2}\left|\boldsymbol{U}_{\rm pq}\right|^2 \int \exp[-{\rm i}Q_x x] \times \exp[-Q_z^2\sigma_0^2(1-\rho(x,t))]{\rm d}x, \quad (10)$$

where σ_0^2 is the variance of the large-scale sea surface roughness and $\rho(x,t)$ denotes the correlation coefficient as a function of the time from a given state, $\{Q_x,\ Q_z,\ Q\}$ are defined as

$$Q_x = k(\sin\theta_{\rm s} - \sin\theta_{\rm i}), \quad (11)$$

$$Q_z = k(\cos\theta_{\rm s} + \cos\theta_{\rm i}), \quad (12)$$

$$Q = \sqrt{Q_x^2 + Q_z^2}. \quad (13)$$

In the high-frequency limit, i.e., $Q_z^2\sigma_0^2 \to \infty$, the integrand in Eq. (10) is highly peaked when $x \to 0$ and $t \to 0$. Thus the correlation coefficient $\rho(x,t)$ can be expanded as a Taylor series in short lag $\{x,\ t\}$, i.e.

$$\rho(x,t) \approx 1 + \rho_{xx}x^2 + \rho_{tt}t^2 + \rho_{xt}xt, \quad (14)$$

where ρ_{xx}, ρ_{tt} and ρ_{xt} are related to the derivatives of the correlation coefficient $\rho(x,t)$ evaluated at zero lag,

$$\rho_{xx} = \frac{1}{2}\frac{\partial^2\rho(x,t)}{\partial x^2}\bigg|_{x=t=0}, \quad (15)$$

$$\rho_{tt} = \frac{1}{2}\frac{\partial^2\rho(x,t)}{\partial t^2}\bigg|_{x=t=0}, \quad (16)$$

$$\rho_{xt} = \frac{\partial^2\rho(x,t)}{\partial x\partial t}\bigg|_{x=t=0}. \quad (17)$$

The integration limits in Eq. (10) may be extended to infinity with negligible error so long as the scattering region contains several correlation lengths of the surface roughness. Substituting Eqs. (11)–(14) into Eq. (10), the indicated integration may then be performed immediately, yielding

$$\begin{aligned}\sigma_{\rm pq} &= \frac{kQ^2}{4Q_z^2}\left|\boldsymbol{U}_{\rm pq}\right|^2 \exp(Q_z^2\sigma_0^2\rho_{tt}t^2)\int \exp[-{\rm i}Q_x x]\exp[Q_z^2\sigma_0^2(\rho_{xx}x^2+\rho_{xt}xt)]{\rm d}x \\ &\approx \frac{kQ^2}{4Q_z^2}\left|\boldsymbol{U}_{\rm pq}\right|^2 \exp(Q_z^2\sigma_0^2\rho_{tt}t^2)\int [\cos(Q_x x) - {\rm i}\sin(Q_x x)]\exp[Q_z^2\sigma_0^2(\rho_{xx}x^2+\rho_{xt}xt)]{\rm d}x \\ &= \frac{\sqrt{\pi}k^2Q^2}{4Q_z^3\sigma_0}\left|\boldsymbol{U}_{\rm pq}\right|^2\sqrt{\frac{-1}{\rho_{xx}}}\exp\left(\frac{Q_x^2}{4Q_z^2\sigma_0^2\rho_{xx}}\right)\exp(\xi t^2 + {\rm i}2\pi f_{\rm D}t), \end{aligned} \quad (18)$$

where

$$\xi = Q_z^2\sigma_0^2\rho_{tt} - \frac{Q_z^2\sigma_0^2\rho_{xt}^2}{4\rho_{xx}}, \quad (19)$$

and the Doppler shift of the scattered field is

$$f_{\rm D} = \frac{Q_x\rho_{xt}}{4\pi\rho_{xx}}. \quad (20)$$

To derive Eq. (18), the following two integral formulas have been utilized:[13]

$$\int_{-\infty}^{+\infty}\cos(2qx)\exp(-ax^2-2bx){\rm d}x = \sqrt{\frac{\pi}{a}}\exp\left(\frac{b^2-q^2}{a}\right)\cos\left(-\frac{2bq}{a}\right), \quad a>0, \quad (21)$$

$$\int_{-\infty}^{+\infty}\sin(2qx)\exp(-ax^2-2bx){\rm d}x = \sqrt{\frac{\pi}{a}}\exp\left(\frac{b^2-q^2}{a}\right)\sin\left(-\frac{2bq}{a}\right), \quad a>0. \quad (22)$$

3. Spectral bandwidth of scattered field

Doppler bandwidth f_δ, i.e. the second moment of the Doppler spectrum, can be defined as[2,14]

$$f_\delta^2 = \frac{\langle f^2\sigma_{\rm pq}\rangle}{\langle\sigma_{\rm pq}\rangle} - \left[\frac{\langle f\sigma_{\rm pq}\rangle}{\langle\sigma_{\rm pq}\rangle}\right]^2, \quad (23)$$

where f and $\sigma_{\rm pq}$ denote the Doppler frequency and the NRCS of each scattering facet, respectively. $\langle\cdot\rangle$ indicates an ensemble average. Neglecting the influence of the hydrodynamic modulation, we may assume that the scattered fields from the regions around the specular points make the same contributions to the NRCS of the sea surface. As mentioned above, the specular points are determined only by incidence and scattering angles, and the slopes of the regions around the specular points are the same. Thus such an assumption is reasonable. With this assumption, equation (23) can be rewritten as

$$f_\delta^2 = \left\langle f^2 \right\rangle - \left[\langle f \rangle\right]^2 = \frac{4}{\lambda^2}\left\{\left\langle V^2 \right\rangle - \left[\langle V \rangle\right]^2\right\} \tag{24}$$

with

$$V = u_x \sin\theta_{\rm i} + u_z \cos\theta_{\rm i}, \tag{25}$$

where λ is the wavelength of the incident radar wave, u_x and u_z denote the velocity components of the orbit movement along the x and the z directions, respectively. Averaging over the statistical ensemble of scattering facets obviously results in the following equation for the bandwidth of Doppler spectrum:

$$f_\delta^2 = \frac{4}{\lambda^2}\left\{\int (u_x \sin\theta_{\rm i} + u_z \cos\theta_{\rm i})^2 P_{\rm s}(u_x, u_z){\rm d}u_x{\rm d}u_z - \left[\int (u_x \sin\theta_{\rm i} + u_z \cos\theta_{\rm i}) P_{\rm s}(u_x, u_z){\rm d}u_x{\rm d}u_z\right]^2\right\}, \tag{26}$$

where $P_{\rm s}(u_x, u_z)$ represents the conditional probability density function of the orbit velocities and it can be determined by the joint probability density function of the slope s and the orbital velocity $\{u_x, u_z\}$. Technically, it is convenient to represent the joint probability density function $P(s, u_x, u_z)$ in terms of corresponding characteristic function $\tilde{P}(\xi, \zeta_x, \zeta_z)$, i.e.

$$P(s, u_x, u_z) = \frac{1}{(2\pi)^3}\iiint \tilde{P}(\xi, \zeta_x, \zeta_z)\exp({\rm i}\xi s + {\rm i}\zeta_x u_x + {\rm i}\zeta_z u_z){\rm d}\xi{\rm d}\zeta_x{\rm d}\zeta_z. \tag{27}$$

In the case of the sea surface, it is simple to obtain explicit results on the assumption that the surface heights are Gaussian statistics. In this case, $\tilde{P}(\xi, \zeta_x, \zeta_z)$ is determined completely by correlation functions of slope and orbital velocities as[15]

$$\tilde{P}(\xi, \zeta_x, \zeta_z) = \exp\left\{-\frac{1}{2}\sigma_{\rm s}^2\xi^2 - \frac{1}{2}\sigma_{ux}^2\zeta_x^2 - \frac{1}{2}\sigma_{uz}^2\zeta_z^2 - \langle su_x\rangle\,\xi\zeta_x - \langle su_z\rangle\,\xi\zeta_z - \langle u_x u_z\rangle\,\zeta_x\zeta_z\right\}, \tag{28}$$

where $\sigma_{\rm s}^2$ and $\sigma_{u\alpha}^2$ are variance of slope and of α component of orbital velocity (u_x, u_z), respectively. Also here, we have correlations between slope s and some u components. For one-dimensional linear sea surface, the variances and the correlation functions can be computed as moments of the sea surface spectrum[5,6] through the relations

$$\sigma_{\rm s}^2 = \int K_x^2 W(K_x){\rm d}K_x, \tag{29}$$

$$\sigma_{ux}^2 = \sigma_{uz}^2 = g\int |K_x|\, W(K_x){\rm d}K_x, \tag{30}$$

and

$$\langle su_z\rangle = -\sqrt{g}\int |K_x|^{3/2}\, W(K_x){\rm d}K_x. \tag{31}$$

For a linear sea surface, $\langle su_x\rangle = \langle u_x u_z\rangle = 0$. And then equation (28) is simplified into

$$\tilde{P}(\xi, \zeta_x, \zeta_z) = \exp\left\{-\frac{1}{2}\sigma_{\rm s}^2\xi^2 - \frac{1}{2}\sigma_{ux}^2\zeta_x^2 - \frac{1}{2}\sigma_{uz}^2\zeta_z^2 - \langle su_z\rangle\,\xi\zeta_z\right\}. \tag{32}$$

Substituting Eq. (32) into Eq. (27) and performing the integration, we can obtain the expression for the joint probability density function as

$$P(s, u_x, u_z) = \left(\sqrt{8\pi^3\sigma_{ux}^2\sigma_{\rm s}^2\left(\sigma_{uz}^2 - \frac{\langle su_z\rangle^2}{\sigma_{\rm s}^2}\right)}\right)^{-1}\exp\left(-\frac{u_x^2}{2\sigma_{ux}^2} - \frac{s^2}{2\sigma_{\rm s}^2} - \frac{\left(u_z - \dfrac{\langle su_z\rangle}{\sigma_{\rm s}^2}s\right)^2}{2\left(\sigma_{uz}^2 - \dfrac{\langle su_z\rangle^2}{\sigma_{\rm s}^2}\right)}\right). \tag{33}$$

Using Eq. (33), the conditional probability of u_x and u_z is then obtained as

$$\begin{aligned} P_{\rm s}(u_x,u_z) &= P(u_x,u_z,|s) \\ &= \frac{P(s,u_x,u_z)}{P(s)} \\ &= \left(\sqrt{4\pi^2\sigma_{ux}^2\left(\sigma_{uz}^2-\frac{\langle su_z\rangle^2}{\sigma_{\rm s}^2}\right)}\right)^{-1} \exp\left(-\frac{u_x^2}{2\sigma_{ux}^2}-\frac{\left(u_z-\frac{\langle su_z\rangle}{\sigma_{\rm s}^2}s\right)^2}{2\left(\sigma_{uz}^2-\frac{\langle su_z\rangle^2}{\sigma_{\rm s}^2}\right)}\right), \end{aligned} \tag{34}$$

where $P(s)=\left(\sqrt{2\pi\sigma_{\rm s}^2}\right)^{-1}\exp\left[-s^2/(2\sigma_{\rm s}^2)\right]$ is the probability function of sea surface slope.[16]

Substituting Eq. (34) into Eq. (26) and performing the integration, after some manipulations, Doppler bandwidth f_δ is obtained as

$$f_\sigma=\frac{2}{\lambda}\sqrt{\left[\sigma_{ux}^2\sin^2\theta_{\rm i}+\cos^2\theta_{\rm i}\left(\sigma_{uz}^2-\frac{\langle su_z\rangle^2}{\sigma_{\rm s}^2}\right)\right]}. \tag{35}$$

4. Numerical results

The predicted Doppler shifts and bandwidths are presented in Figs. 1 and 2 respectively for various radar frequencies. Here, the incidence angle is equal to 5°. For comparison, the simulated results related to the TSM[1] and the exact numerical method[17] (MOM) are also presented. From Figs. 1 and 2, it is obvious that the results predicted by our formulas fit to the accurate numerical results much better than the results obtained by the TSM. This is because at small incidence angles the Doppler spectral model given by the TSM is insufficient.

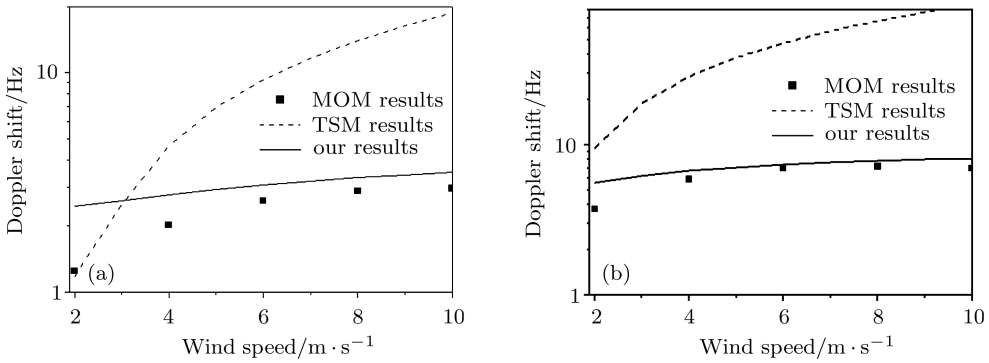


Fig. 1. Doppler shifts versus wind speed for radar frequency $f_{\rm e}=1.3$ GHz (a) and 5.3 GHz (b).

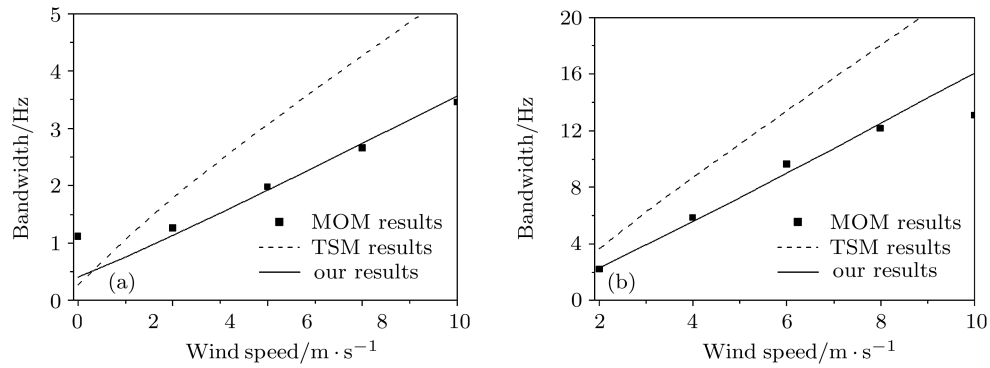


Fig. 2. Bandwidths versus wind speed for radar frequency $f_{\rm e}=1.3$ GHz (a) and 5.3 GHz (b).

As shown in Fig. 1, we can obtain an impression that Doppler shifts do increase with the wind speed at the speed range (2 ∼10 m/s) and the increasing rate decreases at high wind speeds. From Fig. 2, it is found that spectral width is proportional to wind speed approximately. As shown both in Fig. 1(a) and in Fig. 2(a), the differences between our results and the simulations by MOM are noticeable at low wind speeds. This disagreement is mainly due to the fact that at low wind speeds the sea surface roughness is small and the tangential fields cannot be evaluated accurately from Eqs. (4) and (5).

In Fig. 3, Doppler parameters (Doppler shift and bandwidth) each as a function of radar frequency are presented. Here, the wind speed is 5 m/s and the incidence angle equals 5°. As shown in Fig. 3, the Doppler shift and the bandwidth are both increasing with the increase of radar frequency. And the results predicted by our model are in agreement with those obtained by the MOM.

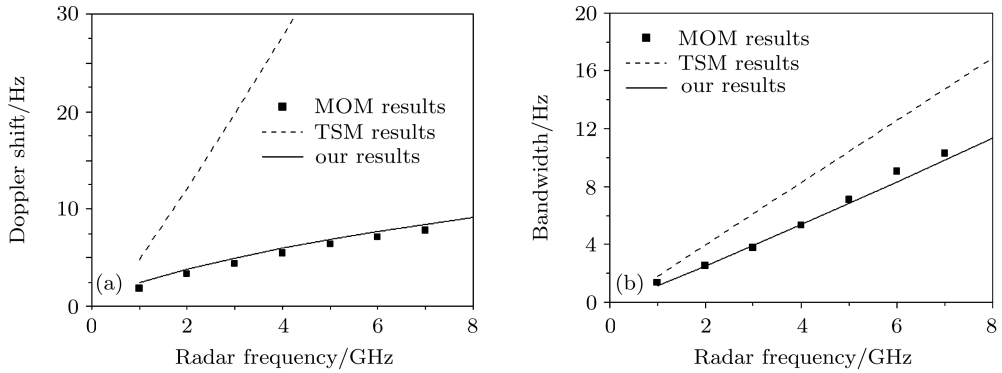


Fig. 3. Comparisons among curves for Doppler parameters (Doppler shift (a) and bandwidth (b)) predicted by different methods versus radar frequency.

The predicted Doppler shifts and bandwidths each as a function of incidence angle for different radar frequencies are illustrated in Figs. 4 and 5, respectively. From Fig. 4, we can find that the predicted Doppler shift increases with the incidence angle increasing from 0° to 10°. And the agreement with the numerical simulation results both at L- and C-bands seems to be quite good. From Fig. 5, it is obvious that the bandwidths corresponding to our model and the numerical simulations show good agreement at smaller incidence angles ($\theta_{\rm i} \leq 5°$). However, at the incidence angles ranging from 5° to 10°, the bandwidths obtained from direct numerical simulations are significantly larger than the predictions of our model. This is because not only the specular points but also the other scattering points on the time-varying sea surface can make significant contributions to spectral width at larger incidence angles. Therefore, reasonable results could be obtained from our formula only when the incidence angle is smaller than 5°.

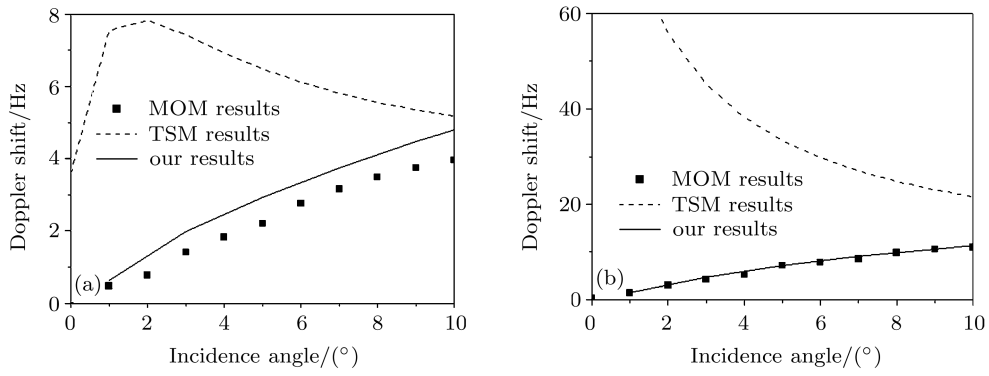


Fig. 4. Doppler shifts versus incidence angle for 5 m/s sea surface and radar frequency $f_{\rm e} = 1.3$ GHz (a) and 5.3 GHz (b).

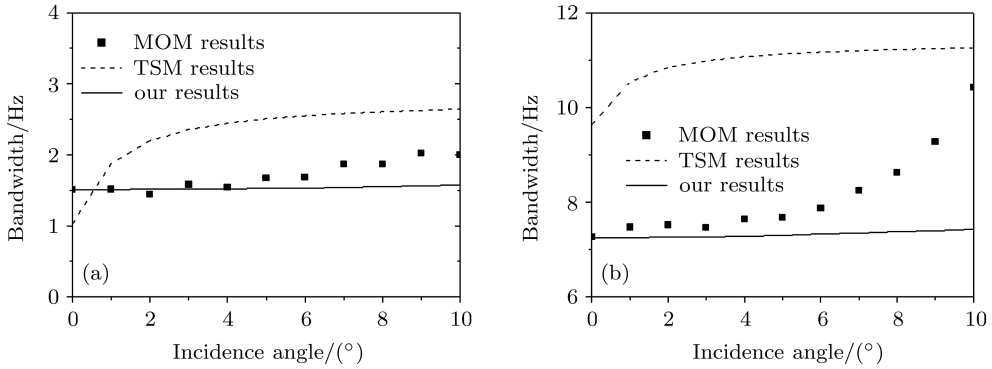


Fig. 5. Bandwidths versus incidence angle for 5 m/s sea surface and radar frequency f_e = 1.3 GHz (a) and 5.3 GHz (b).

5. Conclusions

In this work, the formulas for Doppler parameters (Doppler shift and bandwidth) of specular point scattering from time-varying sea surface are derived in combination with the Kirchhoff approach and the stationary phase approximation. The comparisons between the results predicted by our formulas and the direct numerical simulations show that our proposed formulas hold for the specular point scattering case. Meanwhile, it is found that the Doppler parameters are dependent on radar frequency, wind speed, and incidence angle. The Doppler shift and the bandwidth both turn larger with the increase of wind speed and radar frequency. By comparison with numerical simulations, we also point out that the applicable range of our formula for spectral width is $\theta_i \leq 5°$.

Although this work is limited to the case of the 1D sea surface, the conclusions obtained in this work seem promising for a better understanding of the Doppler spectra of the specular point scattering fields from time-varying sea surfaces.

References

[1] Romeiser R and Thompson D R 2000 *IEEE Trans. Geosci. Remote Senging* **38** 446

[2] Keller M S, Plant W J, Petitt R A and Terray E A 1994 *J. Geophys. Res.* **99** 9751

[3] Johannessen J A, Chapron B, Collard F, Kudryavtsev V, Mouche A, Akimov D and Dagestad K F 2008 *J. Geophys. Res. Lett.* **35** 1

[4] Hayslip A R, Johnson J T and Baker G R 2003 *IEEE Trans. Geosci. Remote Sensing* **41** 2287

[5] Johnson J T, Toporkov J V and Brown G S 2001 *IEEE Trans. Geosci. Remote Sensing* **39** 2411

[6] Toporkov J V and Brown G S 2000 *IEEE Trans. Geosci. Remote Sensing* **38** 1616

[7] Mouche A A, Chapron B, Reul N and Collard F 2008 *Waves in Random and Complex Media* **18** 185

[8] Guo L X, Wang R, Wang Y H and Wu Z S 2008 *Acta Phys. Sin.* **56** 3464 (in Chinese)

[9] Zhang Y M, Wang Y H and Guo L X 2010 *Chin. Phys.* **B 19** 054103

[10] Guo L X, Wang Y H and Wu Z S 2005 *Acta Phys. Sin.* **54** 96 (in Chinese)

[11] Zavorotny V U and Voronovich A G 1998 *IEEE Trans. Antennas Propagat.* **46** 84

[12] Ulaby F T, Moore R K and Fung A K 1982 *Microwave Remote Sensing.* Vol. 2 Chap. 12 (Bostom: Addison-Wesley Publishing Company)

[13] Gradshteyn I S and Ryzhik I M 1980 *Table of Integrals, Series and Products* (Burlington: Academic Press)

[14] Longuet-Higgins M S 1975 *J. Geophys. Res.* **80** 2688

[15] Bisgaard T M and Sasvari Z 2000 *Characteristic Functions and Moment Sequences* (New York: Nova Science Publishers)

[16] Xu D L and Yu D Y 2001 *Theory of Random Ocean Waves* (Beijing: Higher Education Press) (in Chinese)

[17] Franceschetti G, Iodice A and Riccio D 2000 *IEEE Trans. Antennas Propagat.* **38** 1644